Ballistic Track Initialization from a Bisatellite Surveillance Imaging System

Jean Dezert
Onera, DTIM Department,
29 Av. Division Leclerc, 92320 Châtillon, France.
Jean.Dezert@onera.fr

Abstract – *This paper presents a new approach for ballistic target detection and tracking based on delocalized bisatellite surveillance system. The basic idea for track initialization is to use the advantage of stereovision provided by the two imaging IR sensors aboard surveillance geostationary satellites to improve the quality of the true target track detection and to reduce the number of false track initializations. Two methods are presented in the paper. The first method is based on a pixel matching technique using the principle of stereovision. The second and simpliest method is based on the matching of local 2D tracks initialized by a classical* $(2/2)(M/N)$ *Markov-chain logic on each focal plane of imaging with a proper thresholding technique for track elimination based on physical constraints on 3D track. Some examples of bisatellite ballistic track initialization are given and the comparison of the two proposed solutions developed is discussed.*

Keywords: Tracking, track formation, image fusion, ballistic target, cascaded logic, satellite surveillance.

1 Introduction

Surveillance of targets from infrared (IR) satellite observations is a major concern for modern defense systems, especially for the detection and tracking of dim ballistic missiles and estimation of the launching site position to identify as quickly as possible the origin of the threat. In such systems, track formation (or track initialization) is a crucial phase. The surveillance from space by only one single imaging sensor does not allow the full estimation of the 3D trajectory. It is necessary to use at least two delocalized satellites (properly located and focalized towards the same surveillance area) two obtain the 3D estimation of the target kinematics parameters (position, velocity, acceleration, etc). We consider here the simpliest system based only on two satellites and called bisatellite tracking system. The difficulty to develop such system, besides the technological and cost considerations, comes from the limited resolution of the IR imaging sensors, possibility of miss detection of target-originated measurements, presence of false alarms due to environmental conditions (cloudy backgrounds), the uncertainty about targets (number of targets, their dynamics and characteristics, etc) and the data association problem. We present here our recent investigations on the development of such tracking system. Our framework is based on the following suboptimal 2-levels methodology. The first level consists to develop good techniques for 2D track initialization for each satellite. The second level consists to consider jointly the 2D tracks as target measurements for a full 3D ballistic tracking filter based on a sharp missile modeling. In the sequel, we focuse our presentation only on level 1 of our methodology. Recent survey papers on ballistic modelings for the development of level 2 can be found in [5]. Two solutions for level 1 implementation are considered. The first solution, based on a pixel matching algorithm is presented in section 2 and the second solution based on a local 2D track matching approach is presented in section 3.

2 The pixel matching solution

The first track initialization method shortly described on figure 1 is based on the search for the matching of pixels corresponding to the target on both satellites observations. The search for pixel matching is solved by using the principle of stereovison [3]. Once the level 1 is done (i.e. the pixel matching is found and the track is initialized by a classical $(2/2)(m/n)$ logic [2]) the 2D matching tracks are sent as measurement to the 3D tracking filter which in charge to estimate the 3D position, velocity and acceleration of the target (level 2). The estimation of 3D target trajectory allows then to estimate the launching site position of the target and to help to identify the origin of the threat.

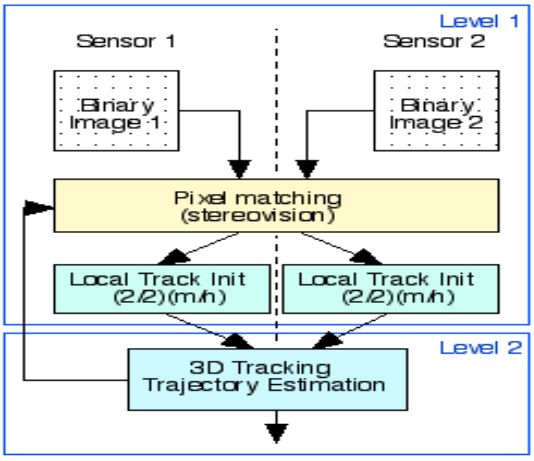

Figure 1: Bisatellite tracking architecture no 1

2.1 Basis of stereovision

Let consider a spatial surveillance system with two delocalized geostationary satellites S_1 and S_2. Each satellite carries its infrared imaging sensor. Both satellites are focalized on the same reference point P_0 at the surface of the earth as described on figure 2.

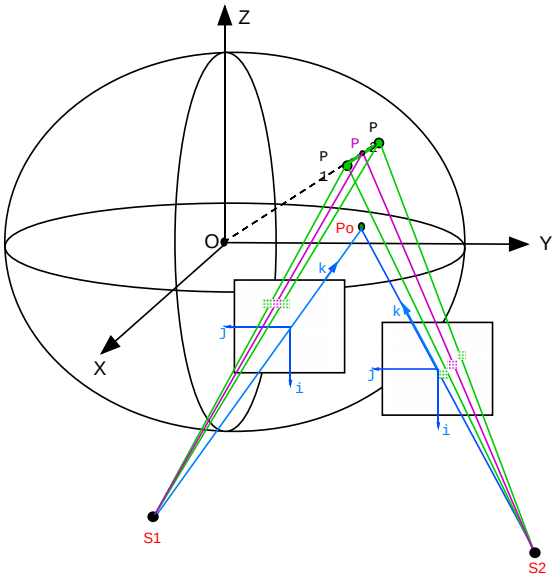

Figure 2: Bisatellite imaging surveillance system

To present the stereovision equations, we assume first that ideal observations conditions are met (i.e. we assume no false alarm, perfect target detection, noise-free target measurements with no bias, same resolution and synchronous observation period for both imaging sensors). We also consider targets as point-target because we consider in this paper that the target size is far smaller than imaging sensor resolution. The 3D position (usually taken at the center of mass of the target) expressed in $(\overrightarrow{Ox}, \overrightarrow{Oy}, \overrightarrow{Oz})$ ECEF (Earth Centered Earth Fixed frame) of a target moving at the surface of the earth and detected in the field ov view of sensors will be denoted P in the sequel. At each observation time t, P admits a projection on the focal plane of each imaging sensor. If one assumes that signal intensities are strong enough to generate the target detection with both satellites, then one will observe the target at a given pixel location on both images (corresponding by example to the purple pixels on figure 2) and thus one gets a stereoscopic observation of the target. The coordinates (u_1, v_1, w_1) of P expressed in the sensor frame T_i associated with a given satellite S are given by

$$\begin{bmatrix} u_1 \\ v_1 \\ w_1 \end{bmatrix} = \mathbf{R}_{T_i}\mathbf{R}_{T_{ned}}\vec{SP}$$

$\mathbf{R}_{T_{ned}}$ is the rotation matrix from the ECEF towards the classical local geographical frame ned (North, East, Down) centered at the location of S. $\mathbf{R}_{T_{ned}}$ is given by the product of the three elementary rotations matrices as follows

$$\mathbf{R}_{T_{ned}} = \mathbf{Rot}_y(-Lat_S)\mathbf{Rot}_x(Long_S)\mathbf{Rot}_y(-\pi/2)$$

where Lat_S and $Long_S$ are the latitude and longitude of satellite S and where rotations matrices $\mathbf{Rot}_x(\alpha)$ and $\mathbf{Rot}_y(\alpha)$ charaterize rotations around axis $\vec{Ox}$ and $\vec{Oy}$ with angle α. $\mathbf{R}_{T_i}$ is the Euler rotation matrix from local frame ned towards sensor frame T_i aiming on the given reference point P_0 located at the surface of the earth. $\mathbf{R}_{T_i}$ is given by

$$\mathbf{R}_{T_i} = \begin{bmatrix} c_\theta c_\psi & c_\theta s_\psi & -s_\theta \\ -s_\psi c_\phi + s_\theta c_\psi s_\phi & s_\theta c_\psi s_\phi + c_\psi c_\phi & c_\theta s_\phi \\ s_\psi s_\phi + s_\theta c_\psi c_\phi & -c_\psi s_\phi + s_\theta s_\psi c_\phi & c_\theta c_\phi \end{bmatrix}$$

c_ψ, c_θ, c_ϕ and s_ψ, s_θ, s_ϕ represent respectively the cosines ans sines of Euler angle ψ, θ and ϕ defining the rotation from ned frame to frame T_i. The aim of an imaging sensor towards P_0 is given by the proper tuning of Euler angles.

Monocular positioning equation

Reciprocally, since $\mathbf{R}_{T_i}^{-1} = \mathbf{R}'_{T_i}$ and $\mathbf{R}_{T_{ned}}^{-1} = \mathbf{R}'_{T_{ned}}$, $\vec{SP}$ can be expressed as function of target coordinates

in imaging frame T_i as

$$\vec{SP} = \mathbf{R}'_{T_{gl}} \mathbf{R}'_{T_i} \begin{bmatrix} u_1 \\ v_1 \\ w_1 \end{bmatrix} \quad (1)$$

For a satellite S with an imaging sensor with focal f, the target coordinates (u_P, v_P) on image focal plane are theoretically given by

$$u_p = f u_1 / w_1 \qquad v_p = f v_1 / w_1 \qquad w_p \equiv w_1 \quad (2)$$

One has obviously no direct access to the full coordinates (u_1, v_1, w_1) from the imaging system but only to (u_P, v_P) measured on image focal plane. Hence (u_P, v_P) is the only useful information delivered by sensor to help for the target track initialization and tracking. With basic algebraic manipulation, equation (1) can also be rewritten as

$$\vec{SP} = \mid \vec{SP} \mid \begin{bmatrix} a \\ b \\ c \end{bmatrix} \equiv \mu \mathbf{R} \begin{bmatrix} u_P/f \\ v_P/f \\ 1 \end{bmatrix} \quad (3)$$

with $a^2 + b^2 + c^2 = 1$ and

$$\mathbf{R} \triangleq \mathbf{R}'_{T_{gl}} \mathbf{R}'_{T_i} \qquad \mu \triangleq \frac{\mid \vec{SP} \mid}{\sqrt{(u_P/f)^2 + (v_P/f)^2 + 1}}$$

The monocular positioning equation (3) provides the 3D estimation of the position of the target as function of the observed coordinates (u_P, v_P) on the focal plane of the imaging sensor when the focal, the attitude of imaging sensor and the location of S are perfectly known. Note that this equation does not provide the perfect position of the target in general because of the limited resolution of the sensor. This provides the exact position if the projection of P on the focal plane coincides exactly with the center of a pixel of the sensor which is not the case in general. Without the knowledge of one of target coordinates (say z_P), it is easy to check that the complete estimation of 3D position (x_P, y_P, z_P) of the target cannot be achieved from the monocular positioning equation (3) because of constraint $a^2 + b^2 + c^2 = 1$ since one has

$$\mid \vec{SP} \mid = \frac{1}{c}(z_p - z_S)$$

$$x_P = x_S + \mid \vec{SP} \mid a = x_S + \frac{a}{c}(z_p - z_S)$$

$$y_P = y_S + \mid \vec{SP} \mid b = y_S + \frac{b}{c}(z_p - z_S)$$

If one has some prior information about one of the coordinates x_p, y_p or z_p, then the estimation of the 3D position of the target becomes theoretically achievable. This prior knowledge cannot be obtained without addition of a second sensor. Therefore a second imaging sensor is required for the estimation of 3D position of the target.

Stereo positioning equation

We present now the fundamental stereovision positioning equation. The first case presented below assumes the correct pixel matching between images, whereas the second case, involved in practical situations, does not.

Case 1: Stereovision with known pixel matching

Let consider a bisatellite system observing a target P at the surface of the earth corresponding to figure 3. We assume here that the pixel matching between image 1 and 2 is known. In other words, we know that the red pixel on image 1 matches with red pixel on image 2).

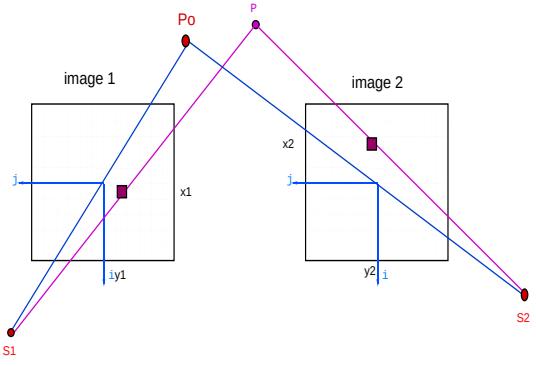

Figure 3: Stereovision with known pixel matching

Under this assumption, the estimation of 3D position of the target P is obtained by solving the overdetermined system of equations

$$\mathbf{A}\mathbf{p} = \mathbf{z} \quad (4)$$

with

$$\mathbf{A} \triangleq \begin{bmatrix} 1 & 0 & -a_1/c_1 \\ 0 & 1 & -b_1/c_1 \\ 1 & 0 & -a_2/c_2 \\ 0 & 1 & -b_2/c_2 \end{bmatrix} \quad \text{and} \quad \mathbf{z} \triangleq \begin{bmatrix} x_{S_1} - a_1 z_{S_1}/c_1 \\ y_{S_1} - b_1 z_{S_1}/c_1 \\ x_{S_2} - a_2 z_{S_2}/c_2 \\ y_{S_2} - b_2 z_{S_2}/c_2 \end{bmatrix}$$

where a_i, b_i, c_i for $i = 1, 2$ are components a,b and c entering in (3) relative to a given satellite S_i. The solution $\hat{\mathbf{p}}$ minimizing the least squares criteria $(\mathbf{A}\mathbf{p} - \mathbf{z})'(\mathbf{A}\mathbf{p} - \mathbf{z})$ and the covariance matrix $\mathbf{P}$ of the estimation error are then given by

$$\hat{\mathbf{p}} = \begin{bmatrix} \hat{x}_P \\ \hat{y}_P \\ \hat{z}_P \end{bmatrix} = [\mathbf{A}'\mathbf{A}]^{-1} \mathbf{A}'\mathbf{z} \quad (5)$$

$$\mathbf{P} = E[(\mathbf{p} - \hat{\mathbf{p}})(\mathbf{p} - \hat{\mathbf{p}})'] = [\mathbf{A}'\mathbf{A}]^{-1} \quad (6)$$

Case 2: Stereovision with unknown pixel matching

The problem of 3D position estimation of P becomes more difficult when the pixel matching is unknown. To estimate P, one has to search for potential pixel matchings between two images by introducing some prior bounds of variation $[z_P^{min}; z_P^{max}]$ on z_P. With such additional constraint as given on figure 4, the pixel $(u_P(S_1), y_P(S_1))$ on image 1 is projected onto a segment (drawn in green color) on image 2 (and reciprocally) following equation

$$u_P(S_2) - u_O(S_2) = \alpha(v_P(S_2) - v_O(S_2))$$

$$\alpha \triangleq [\mathbf{R}_2^{-1}\mathbf{R}_1\mathbf{u}(S_1)]_1/[\mathbf{R}_2^{-1}\mathbf{R}_1\mathbf{u}(S_1)]_2$$

where $[.]_i$ denotes the ith component of the vector into the brackets. $\mathbf{R}_1$ and $\mathbf{R}_2$ correspond to the rotation matrice $\mathbf{R}$ entering in (3) evaluated for satellites S_1 and S_2 and $\mathbf{u}(S_1) \triangleq [u_P(S_1)/f \;\; v_P(S_1)/f \;\; 1]'$. The search for a detection on this segment will provide a potential pixel matching candidate for the estimation of the 3D position of the target with estimation technique described as in previous case. The orientation and the length of the segment depends on the geometry of the problem under consideration (mainly satellites positions and the aim point P_0). More caution must be taken in practice to take into account the possible uncertainty on satellite location, observation noises, etc. Under observation conditions (like heavy cloudy backgrounds), one can also get several detections on a same stereoscopic search segment which yields ambiguities in the pixel matching, or no pixel matching at all sometimes, when the probability of target detection is less than unity. We present on figure 5 a simple illustrating

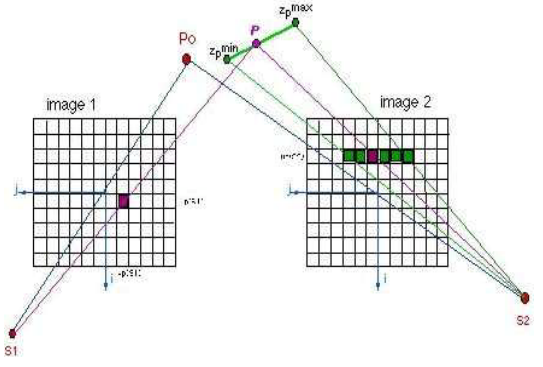

Figure 4: Stereovision with unknown pixel matching

example of a simulated ballistic trajectory (red plot) observed by a bisatellite observation system and the corresponding stereoscopic segments (green plots) associated for an academic assumption $z_P^{min} = z_p - 5$km and $z_P^{max} = z_p + 5$km at each sampling period. This is just an open-loop simulation since we haven't introduced the feedback from the 3D tracker to reduce to stereoscopic search length with time.

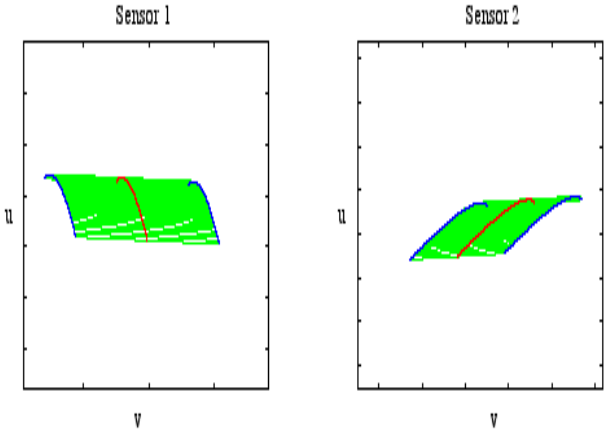

Figure 5: Example of stereoscopic search segment

In short, the general problem of stereovision consists in finding both the potential pixel matching between images and then generates the 3D position measurement for the 3D ballistic tracking filter.

2.2 Influence of attitude noises

The presence of additional attitude noises δ_ψ, δ_θ and δ_ϕ on attitude angles ψ, θ and ϕ yields a noisy target observation. If one assumes zero-mean white gaussian additive attitude noises with given small standard deviations σ_ψ, σ_θ et σ_ϕ, the components r_{ij} of the rotation matrix $\mathbf{R}_{T_i} \triangleq [r_{ij}]$ entering in stereovision equation are given by

$$\begin{aligned}
r_{11} &= c_{\theta+\delta_\theta} c_{\psi+\delta_\psi} \\
r_{12} &= c_{\theta+\delta_\theta} s_{\psi+\delta_\psi} \\
r_{13} &= -s_{\theta+\delta_\theta} \\
r_{21} &= -s_{\psi+\delta_\psi} c_{\phi+\delta_\phi} + s_{\theta+\delta_\theta} c_{\psi+\delta_\psi} s_{\phi+\delta_\phi} \\
r_{22} &= s_{\theta+\delta_\theta} c_{\psi+\delta_\psi} s_{\phi+\delta_\phi} + c_{\psi+\delta_\psi} c_{\phi+\delta_\phi} \\
r_{23} &= c_{\theta+\delta_\theta} s_{\phi+\delta_\phi} \\
r_{31} &= s_{\psi+\delta_\psi} s_{\phi+\delta_\phi} + s_{\theta+\delta_\theta} c_{\psi+\delta_\psi} c_{\phi+\delta_\phi} \\
r_{32} &= -c_{\psi+\delta_\psi} s_{\phi+\delta_\phi} + s_{\theta+\delta_\theta} s_{\psi+\delta_\psi} c_{\phi+\delta_\phi} \\
r_{33} &= c_{\theta+\delta_\theta} c_{\phi+\delta_\phi}
\end{aligned}$$

Using the first-order development of sin and cos functions, one gets for $i = \psi, \theta, \phi$, $s_{i+\delta_i} \approx s_i + c_i\delta_i$ and $c_{i+\delta_i} \approx c_i - s_i\delta_i$ and a first order approximation for $\mathbf{R}_{T_i}$ (not given here explicitly due to space the paper limitation constraint). The expected values $\bar{r}_{ij} = E[r_{ij}]$ of

r_{ij} can then be approximated by

$$\begin{aligned}
\bar{r}_{11} &= c_\theta c_\psi \\
\bar{r}_{12} &= c_\theta s_\psi \\
\bar{r}_{13} &= -s_\theta \\
\bar{r}_{21} &= -s_\psi c_\phi + s_\theta c_\psi s_\phi \\
\bar{r}_{22} &= s_\theta c_\psi s_\phi + c_\psi c_\phi \\
\bar{r}_{23} &= c_\theta s_\phi \\
\bar{r}_{31} &= s_\psi s_\phi + s_\theta c_\psi c_\phi \\
\bar{r}_{32} &= -c_\psi s_\phi + s_\theta s_\psi c_\phi \\
\bar{r}_{33} &= c_\theta c_\phi
\end{aligned}$$

The variances $\sigma^2_{r_{ij}} = E[(r_{ij} - \bar{r}_{ij})(r_{ij} - \bar{r}_{ij})]$ and cross-correlation terms $\sigma^2_{r_{ij}r_{kl}} = E[(r_{ij} - \bar{r}_{ij})(r_{kl} - \bar{r}_{kl})]$ can be easily derived and correspond to the components of the following 9×9 covariance matrix

$$\mathbf{P_{rr}} = E[(\mathbf{r} - \bar{\mathbf{r}})(\mathbf{r} - \bar{\mathbf{r}})'] = \begin{bmatrix} P_{\mathbf{r}_1\mathbf{r}_1} & P_{\mathbf{r}_1\mathbf{r}_2} & P_{\mathbf{r}_1\mathbf{r}_3} \\ P_{\mathbf{r}_2\mathbf{r}_1} & P_{\mathbf{r}_2\mathbf{r}_2} & P_{\mathbf{r}_2\mathbf{r}_3} \\ P_{\mathbf{r}_3\mathbf{r}_1} & P_{\mathbf{r}_3\mathbf{r}_2} & P_{\mathbf{r}_3\mathbf{r}_3} \end{bmatrix}$$

with

$$\begin{cases} \mathbf{r}_1 \triangleq [r_{11}\ r_{12}\ r_{13}]' \\ \mathbf{r}_2 \triangleq [r_{21}\ r_{22}\ r_{23}]' \\ \mathbf{r}_3 \triangleq [r_{31}\ r_{32}\ r_{33}]' \end{cases} \qquad \mathbf{r} \triangleq \begin{bmatrix} \mathbf{r}'_1 \\ \mathbf{r}'_2 \\ \mathbf{r}'_3 \end{bmatrix} \qquad \bar{\mathbf{r}} \triangleq E[\mathbf{r}]$$

The introduction of attitude noises into Euler matrix $\mathbf{R}_{T_i}$ generates directly errors on target position $\mathbf{u} = [u_1, v_1, w_1]'$ in frame T_i under consideration. Actually, for a given vector $\vec{SP}$ and for small gaussian attitude noises, it can be shown that $\mathbf{u}$ follows a gaussian distribution $\mathcal{N}(\bar{\mathbf{u}}, \mathbf{P_{uu}})$ with mean $\bar{\mathbf{u}} = E[\mathbf{u}] = [\mathbf{x}'\bar{\mathbf{r}}_1\ \mathbf{x}'\bar{\mathbf{r}}_2\ \mathbf{x}'\bar{\mathbf{r}}_3]'$ and variance $\mathbf{P_{uu}} = [\mathbf{x}'\mathbf{P}_{\mathbf{r}_i\mathbf{r}_j}\mathbf{x}]$ where $\mathbf{x} \triangleq \mathbf{R}_{T_{gl}}\vec{SP}$. More precisely,

$$\mathbf{P_{uu}} = \begin{bmatrix} \mathbf{x}'P_{\mathbf{r}_1\mathbf{r}_1}\mathbf{x} & \mathbf{x}'P_{\mathbf{r}_1\mathbf{r}_2}\mathbf{x} & \mathbf{x}'P_{\mathbf{r}_1\mathbf{r}_3}\mathbf{x} \\ \mathbf{x}'P_{\mathbf{r}_2\mathbf{r}_1}\mathbf{x} & \mathbf{x}'P_{\mathbf{r}_2\mathbf{r}_2}\mathbf{x} & \mathbf{x}'P_{\mathbf{r}_2\mathbf{r}_3}\mathbf{x} \\ \mathbf{x}'P_{\mathbf{r}_3\mathbf{r}_1}\mathbf{x} & \mathbf{x}'P_{\mathbf{r}_3\mathbf{r}_2}\mathbf{x} & \mathbf{x}'P_{\mathbf{r}_3\mathbf{r}_3}\mathbf{x} \end{bmatrix}$$

From the known distribution $p(\mathbf{u}) = \mathcal{N}(\bar{\mathbf{u}}, \mathbf{P_{uu}})$, we would like to obtain the density of the observation $\mathbf{u}_P = [u_P\ v_P\ w_P]' \triangleq [uf/w\ v_f/w\ w]'$ or at least the two first moments of this distribution. From Hinkley's result [4], one knows that the density $p(r)$ of the ratio $r = \alpha/\beta$ of two jointly gaussian random variables α and β with means μ_1,μ_2, and variances σ_1^2, σ_2^2 and with correlation factor ρ is given by

$$\begin{aligned} p(r) = &\frac{\sqrt{1-\rho^2}}{\pi\sigma_1\sigma_2 a^2(r)}\exp(-\frac{c}{2(1-\rho^2)}) \\ &+\frac{b(r)d(r)}{\sqrt{2\pi\sigma_1\sigma_2 a^3(r)}}\Big[\Phi(\frac{b(r)}{a(r)\sqrt{1-\rho^2}}) \\ &-\Phi(-\frac{b(r)}{a(r)\sqrt{1-\rho^2}})\Big] \end{aligned}$$

where $\Phi(.)$ denotes the cdf of normal density and where coefficients $a(r)$, $b(r)$, c and $d(r)$ are given by

$$\begin{aligned} a(r) =& \sqrt{\frac{r^2}{\sigma_2^2} - \frac{2r\rho}{\sigma_1\sigma_2} + \frac{1}{\sigma_1^2}} \\ b(r) =& \frac{r\mu_2}{\sigma_2^2} - \frac{\rho(\mu_2 + \mu_1 r)}{\sigma_1\sigma_2} + \frac{\mu_1}{\sigma_1^2} \\ c =& \frac{\mu_2^2}{\sigma_2^2} - \frac{2\rho\mu_1\mu_2}{\sigma_1\sigma_2} + \frac{\mu_1^2}{\sigma_1^2} \\ d(r) =& \exp\Big[\frac{b^2(r) - ca^2(r)}{2(1-\rho^2)a^2(r)}\Big] \end{aligned}$$

Although the density $p(r)$ is well defined, all the statistical moments of r do not exist since the integrals $\int r^n p(r)dr$ are not defined. In practice however, the density $p(\mathbf{u})$ is not exactly gaussian (it is only gaussian at first order approximation), thus the density of components u_P and v_P of $\mathbf{u}_P$ does not correspond exactly to the density $p(r)$ but the first and second moments can be approximated by the first order linearization of vector $\mathbf{u}_P + \delta\mathbf{u}_P = [u_P + \delta_u\ v_P + \delta_v\ w_P + \delta_w]'$. Then, one gets the following approximations

$$\begin{aligned} \bar{u}_P &= E[u_P] \approx f\bar{u}/\bar{w} \\ \bar{v}_P &= E[v_P] \approx f\bar{v}/\bar{w} \\ \bar{w}_P &= E[w_P] \approx \bar{w} \\ \mathbf{P}_{u_P,v_P,w_P} &\approx \mathbf{H}\mathbf{P_{uu}}\mathbf{H}' \end{aligned}$$

with

$$\mathbf{H} = \begin{bmatrix} f/\bar{w} & 0 & -f\bar{u}/\bar{w}^2 \\ 0 & f/\bar{w} & -f\bar{v}/\bar{w}^2 \\ 0 & 0 & 1 \end{bmatrix}$$

Extensive Monte-Carlo simulations based on several simulated ballistic trajectories for different scenarios and different geostationary satellite positionings have shown a very good agreement of the approximation proposed here. The attitude noises on target measurements can therefore be taken into account explicitly to evaluate the covariance matrix $\mathbf{R}$ of target measurements (as presented in figure 6). This will allow us to set up a theoretical (stereoscopic) measurement validation technique (gating) for our new pixel-based bisatellite tracking filter.

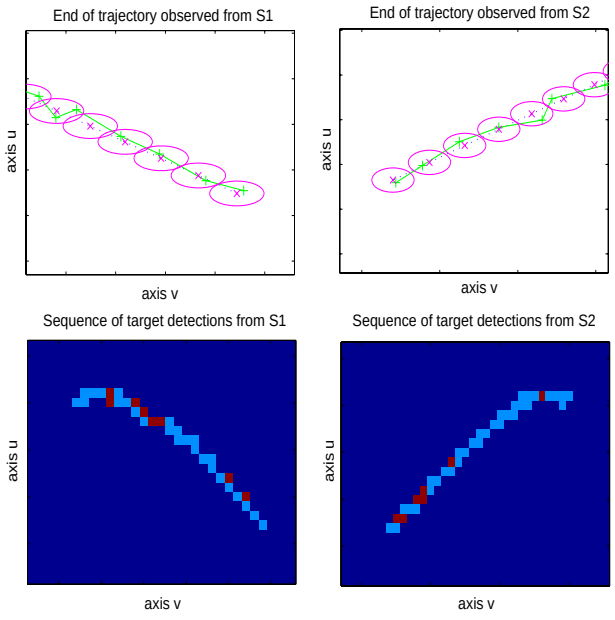

Figure 6: Influence of attitude noises on observation

2.3 Influence of attitude biases

The existence of an unknown bias on satellite attitude ψ, θ and ϕ modifies the value of the rotation matrix $\mathbf{R}_T$, and can yield to dramatical effects on tracking performances. The biases must be estimated and removed before observations processing. Without extra specific devices (like a precise stellar and/or landmark positioning system to estimate satellite attitude), there is however no theoretical method to estimate such biases from IR image provided by the imaging sensor itself. The reliability of the surveillance system therefore highly depends on the quality of the sensor unbiasness which cannot be achieved without a (costly) sophisticated technological solution unless if the level of bias is very small with respect to sensor resolution.

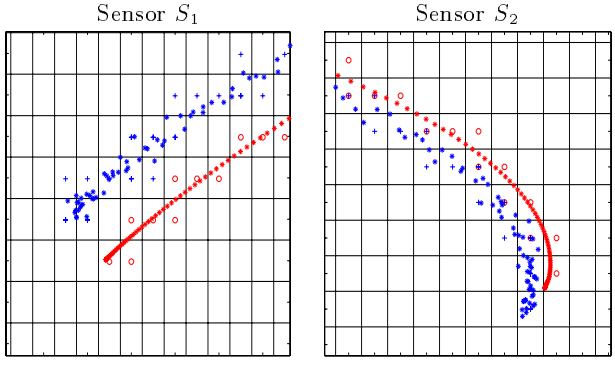

Figure 7: Bias effects on target observation

We show on figure 7 for a given image resolution with few micro radians of standard deviation for observation noises and few ten or so micro radians of bias on ψ, θ and ϕ, the effects of biases on the target observation. For each sensor, the red plots indicates the true trajectory as it should be observed in the bias-free case and the corresponding centers for pixel detections (o). The blue plots indicate the observed trajectory with bias effects and the centers of pixel detections (+). The black grid indicates the limit of the pixels of the images. One can easily see the dramatic effects of the bias on the observed target trajectory.

2.4 Summary of the method

Here is briefly the main seven steps involved in the level 1 phase of the bisatellite tracking system based on pixel matching approach.

1. Start with each detection d_i^1 on image S_1 and choose initial bounds of possible altitude for the target.

2. From each d_i^1, look for corresponding pixel d_j^2 on image S_2 using stereo searching constraint described in section 2.1. All pairs of pixels (d_i^1, d_j^2) become potential bisatellite track initiators.

3. Use the standard $(2/2)(m/n)$ Markov-chain logic [1, 2] to initialize 2D local tracks for each sensor. Use the constant velocity model for the two first detections and a constant acceleration model as soon as 3 detections in the chain is available.

4. When one has prior information on the maximal admissible velocity of the target under consideration, one can reduce drastically the number of false tracks by eliminating all chains for which the distances between two consecutive detections in the focal planes are above a given threshold.

5. Give each admissible pair of local tracks (i.e pairs of tracks based on pairs of matched pixels satisfying the previous constraint) to level 2 (3D tracking filter based on sharp missile model).

6. Estimate the 3D trajectories and eliminate all pairs of tracks given rise to incompatible trajectories based on physical criterias (corresponding for example of targets having negative climbing speed).

7. For each remaining 3D track, predict the altitude of the targets for the next observation period and go back to step 2.

2.5 Simulation examples

The figure 8 shows a typical example of a pixel matching result at a given observation period. The detections available from each satellite are plotted in red on top subplots and in black dots on bottom subplots. Only one target has been introduced in this scenario and appears at the bottom of images (blue star). The result of the stereo matching search is given on the two subplots on the figure (red circles) at the bottom of the figure. The pair of pixel corresponding to the target has been selected among the set of all possible admissible pairs. This set of pairs of pixels will serve to update 2D track initialization process.

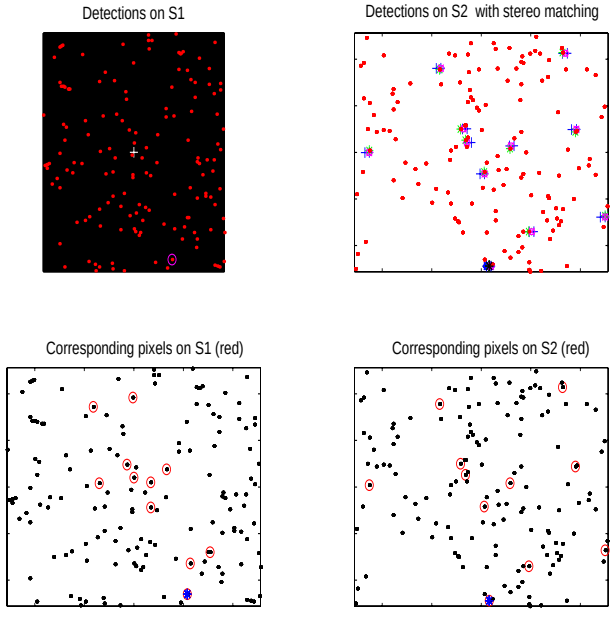

Figure 8: Typical example of the pixel matching

The figure 9 shows a typical result of the target track initialization process based on the stereo pixel matching technique coupled with a $(2/2)(3/4)$ sliding track formation logic during 10 observation periods. Blue stars indicate the chain of detections whereas black squares indicate the filtered 2D trajectories for both sensors. Monte-Carlo simulations have shown that the performances of this technique depends highly on the level of target detection probabilities, the precision and the unbiasness of the estimation of the altitude of the targets. The major drawbacks of this solution is its heavy computational burden required for the stereo-vision pixel matching search and the necessity of synchronous observations.

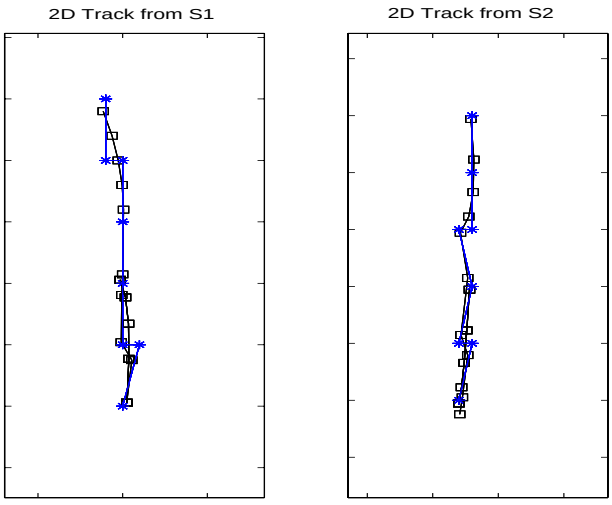

Figure 9: Typical example of 2D track initialization

3 The track matching solution

To overcome the drawbacks of the pixel mtaching solution, we propose now the second solution based on the 2D Track matching method schematically described on figure 10. The simple basic idea of this 2 levels approach is first to initialize 2D track with a classical $(2/2)(m/n)$ logic [2] for each satellite and then for each possible pair of 2D local track, one estimates the corresponding evolution of the altitude of the target and its climbing speed. All combinations given rise to unrealistic evolutions are eliminated. Only all the admissible pairs of 2D tracks are provided to the level 2 for full 3D trajectory estimation with the 3D tracking filter. By backward prediction, one can then estimate the launching site position of the target and identify the origin of the threat.

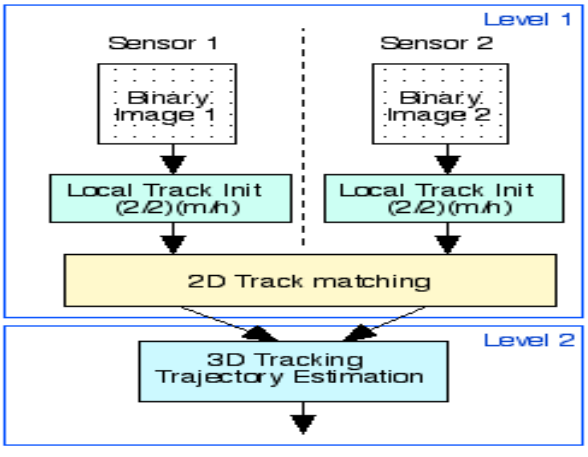

Figure 10: Bisatellite tracking architecture no 2

3.1 Summary of the method

The main steps involved in the level 1 of the bisatellite tracking system based on 2D track matching approach are:

1. Each detection on image S_1 and on image S_2 serves as potential track initiator for each satellite.

2. Use the standard $(2/2)(m/n)$ Markov-chain logic [1, 2] to initialize independently 2D local tracks for each sensor. Use the constant velocity model for the two first detections and a constant acceleration model as soon as 3 detections in the chain is available.

3. Eliminate all the 2D tracks initialized by the logic for which the distances between two consecutive detections in the focal planes are above a given threshold defined by the prior information one has on the maximal admissible speed of the targets.

4. From each combination of pair of local 2D tracks, we estimate the evolution of altitude of the targets during the part of the local tracks having common time stamps. Eliminate all the pairs given rise to unrealistic evolutions (having negative or too high climbing speed, etc). Keep only all admissible pairs of 2D tracks as potential bisatellite set of tracks.

5. Send each admissible pair of local tracks as measurements to level 2 (3D tracking filter based on sharp missile model). Keep tracking by going back to step 2 or project 3D track prediction to each focal plane to update local validated 2D tracks using standard Kalman (or PDAF) filtering.

3.2 Simulation examples

The figure 11 shows a typical result of the bisatellite target track initialization process based on the 2D track matching technique coupled with a $(2/2)(4/6)$ sliding track formation logic during 30 observation periods for a 0.9 target detection probability. Blue stars indicate the chain of detections (center of pixels) whereas black squares indicate the filtered 2D trajectories for both sensors.

4 Conclusion

Two approaches for ballistic target track initialization during the boosted phase from a bisatellite surveillance imaging system have been presented here. The first method based on sterovision and pixel matching technique coupled with a $(2/2)(m/n)$ chain logic requires the synchronism of satellite observations, a high computation burden (when size of images becomes large with a heavy false alarm density) but also a good prior information on the bounds of altitude of the target at the first detection step. To reduce the stereoscopic pixel search area and combinatorics, a feedback of 3D tracking filter at each observation period is also necessary. In our works, we have proved that this first investigated method is actually very delicate to implement with good reliability for a future operational surveillance system. An alternative method based on the matching of local 2D tracks appears more attractive both in terms of computational burden, simplicity of implementation and robustness and also allows to use unsynchronous satellite observations.

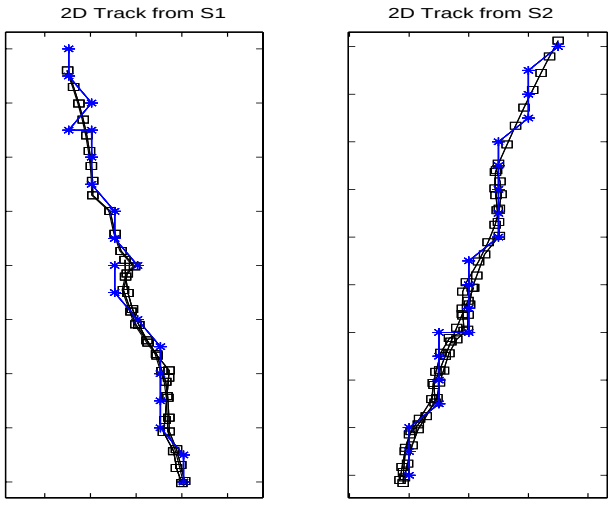

Figure 11: Typical example of 2D track initialization

References

[1] Bar-Shalom Y., Chang K.C., Shertukde H.M. *Performance Evaluation of a Cascaded Logic for Track Formation in Clutter*, IEEE Trans. AES, vol. 25, no 6, pp. 873-878, 1986.

[2] Bar-Shalom Y., Li X.R., *Multitarget-Multisensor Tracking: Principles and Techniques*, YBS Publishing, 1995.

[3] Faugeras O., *Three-Dimensional Computer Vision*, The MIT Press, Cambridge, MA, 1993.

[4] Hinkley D.V., *On the ratio of two correlated normal variables*, Biometrika, 56, pp. 635-639, 1969.

[5] Li X.R., Jilkov V., *A Survey of Maneuvering Target Tracking - Part II:Ballistic Target Models*, Proceedings of SPIE Conference on Signal and Data Processing of Small Targets, Vol. 4473-63, San Diego, CA, USA, Jul-Aug, 2001.